Linear Free Energy Relationships with Quantum Mechanical Corrections: Classical and Quantum Mechanical Rate Constants for Hydride Transfer between NAD^+ Analogues in Solutions

Young Shik Kong[†] and Arieh Warshel*[,‡]

Contribution from the Departments of Chemistry, University of Southern California, Los Angeles, California 90089-1062, and Chonbuk National University, Chonju, Chonbuk 560-756, Korea

Received January 9, 1995[⊗]

Abstract: The microscopic validity of linear free energy relationships for adiabatic reactions in solutions is examined using computer simulation methods and realistic potential surfaces. The simulations consider hydride transfer reactions within a class of NAD^+ analogues. The potential surfaces of the reacting systems are evaluated by the empirical valence bond approach and the corresponding diabatic and adiabatic free energy functions are calculated by a free energy perturbation/umbrella-sampling approach. Quantum mechanical corrections of the activation energies are evaluated by the quantized classical path method. It is demonstrated that a single adjustable parameter that scales the off-diagonal valence bond mixing term reproduces the observed linear free energy relationship with a fully microscopic approach without assuming *a priori* any Marcus-like relationship. Interestingly, the calculated solvent reorganization energies are quite different than those deduced by phenomenological approaches. This reflects the contribution of the solute reorganization energy, the coupling between the diabatic states of the solute, and the effect of quantum mechanical nuclear factors. The present study demonstrates the effectiveness of the empirical valence bond approach for studies of chemical processes in solutions as well as the insight provided by applying the valence bond description to chemical processes in general.

1. Introduction

Computer modeling of the energetics and dynamics of chemical reactions in solutions and proteins recently has become a field of intense activity (see, for example, refs 1−12). The advances in computer power and simulation methods have made it possible to examine fundamental concepts of physical organic chemistry including the microscopic basis of linear free energy relationships (LFER) in solution and in protein active sites.[1a,13] It has been demonstrated, for example, that the solvent contribution to the free energy functions for electron transfer (ET) reactions can be described by quadratic functions.[14−16] This provided a strong support for the validity of the Marcus relationship[17] at a microscopic level. The validity of LFER for adiabatic reactions such as proton transfer (PT), hydride transfer (HT), and other processes has also been examined in a preliminary way.[1,5,13,18] Yet in view of the important rule of LFER in the description of chemical and biological processes (e.g., refs 13 and 19−22) it is important to examine the validity of such relationships in classes of closely related adiabatic reactions. It is important to find out how LFER parameters that are deduced in a phenomenological way from the Marcus formula are related to the corresponding microscopic parameter. It is also important to assess the contribution of quantum mechanical nuclear effects to the observed LFER. The evaluation of such effects can be of particular importance for microscopic analysis of LFER parameters for processes that involve a transfer of light atoms or ions.

The evaluation of quantum mechanical rate constants for chemical reactions in solution is far from being trivial. While simulations of quantum mechanical corrections for diabatic processes such as electron transfer (ET) reactions can be accomplished by well-established methods,[14d,23,24,25] the treatment of such effects in adiabatic reactions presents a major

[†] Chonbuk National University.
[‡] University of Southern California.
[⊗] Abstract published in *Advance ACS Abstracts,* June 1, 1995.

(1) (a) Warshel, A. *Computer Simulation of Chemical Reactions in Enzymes and Solutions*; John Wiley & Sons, Inc.: New York, 1991. (b) Warshel, A.; Levitt, M. *J. Mol. Biol.* **1976**, *103*, 227. (c) Warshel, A. *J. Phys. Chem.* **1982**, *86*, 2218. (d) Aqvist, J.; Warshel, A. *Chem. Rev.* **1993**, *93*, 2523−2544.
(2) Rinaldi, D.; Rivail, J.-L.; Rguini, N. *J. Comput. Chem.* **1992**, *13*, 675.
(3) Tapia, O. *J. Mol. Struct.* **1991**, 226.
(4) Jorgensen, W. L.; Ravimohan, C. *J. Chem. Phys.* **1985**, *83*, 3050.
(5) Hwang, J.-K.; King, G.; Creighton, S.; Warshel, A. *J. Am. Chem. Soc.* **1988**, *110*, 5297.
(6) Singh, U. C.; Kollman, P. A. *J. Comput. Chem.* **1986**, *7*(6), 718.
(7) Bash, P. A.; Field, M. J.; Karplus, M. *J. Am. Chem. Soc.* **1987**, *109*, 8092.
(8) Kim, H. J.; Hynes, J. T. *J. Am. Chem. Soc.* **1992**, *114*, 10508.
(9) Gao, J. *J. Phys. Chem.* **1992**, *96*, 537.
(10) Wang, B.; Ford, G. P. *J. Chem. Phys.* **1992**, *97*, 4162.
(11) Bonaccorsi, R.; Cammi, R.; Tomasi, J. *J. Comput. Chem.* **1991**, *12*, 301.
(12) Warshel, A. In *Structure and reactivity in aqueous solution*; Cramer, C. J., Truhlar, D. G., Eds.; *ACS Symp. Ser.*; American Chemical Society: Washington, DC, 1994; p 568.
(13) (a) Warshel, A.; Hwang, J.-K.; Åqvist, J. *Faraday Discuss.* **1992**, *93*, 225. (b) Warshel, A.; Schweins, T.; Fothergill, M. *J. Am. Chem. Soc.* **1994**, *116*, 8347.
(14) (a) King, G.; Warshel, A. *J. Chem. Phys.* **1990**, *93*, 8682. (b) Warshel, A.; Parson, W. W. *Annu. Rev. Phys. Chem.* **1991**, *42*, 279. (c) Hwang, J.-K.; Warshel, A. *J. Am. Chem. Soc.* **1987**, *109*, 715. (d) Warshel, A.; Hwang, J.-K. *J. Chem. Phys.* **1986**, *84*, 4938.
(15) Kuharski, R. A.; Bader, J. S.; Chandler, D.; Sprik, M.; Klein, M. L.; Impey, R. W. *J. Chem. Phys.* **1988**, *89*, 3248.
(16) Papazyan, A.; Maroncelli, M. *J. Chem. Phys.* **1991**, *95*, 9219.
(17) Marcus, R. A. *Annu. Rev. Phys. Chem.* **1964**, *15*, 155.
(18) Yadav, A.; Jackson, R. M.; Holbrook, J. J.; Warshel, A. *J. Am. Chem. Soc.* **1991**, *113*, 4800.
(19) Hammett, L. P. *Physical Organic Chemistry*; McGraw-Hill: New York, 1990.
(20) Maskill, H. *The Physical Basis of Organic Chemistry*; Oxford University Press: Oxford, U.K., 1985.
(21) Albery, W. J. *Annu. Rev. Phys. Chem.* **1980**, *31*, 227.
(22) Kreevoy, M. M.; Truhlar, D. G. In *Investigation of Rates and Mechanisms of Reactions*; Bernasconi, C. F., Ed.; John Wiley Sons: New York, 1986; Vol. 6, p 13.
(23) Warshel, A.; Chu, Z. T.; Parson, W. W. *Science* **1989**, *246*, 112.

0002-7863/95/1517-6234$09.00/0

computational challenge. Encouraging progress has been made in recent years in studies of adiabatic reactions.[26-31] This includes studies of PT[28,30] and HT[29] reactions in solution by path integral methods and other approaches. It is still not clear, however, how accurate the available methods are. The accuracy problem can be addressed by performing simulations of HT and PT reactions on series of molecules in solution and by comparing the calculated and observed rate constants.

An interesting test case has been provided by the systematic work of Kreevoy and co-workers,[32] who studied hydride transfer reactions in a family of NAD^+ analogues. This class of reactions is the subject of the present work which uses the empirical valence bond (EVB) method[1a,5] to describe the energetics of the HT reactions. This is done by evaluating the classical free energy surfaces by the powerful combination of the EVB with a free energy perturbation/umbrella-sampling method.[1a,5] The quantum mechanical corrections to the classical rate constant are evaluated by our recently developed quantized classical path (QCP) method.[30] This method was already used in studies of HT and PT in solutions and proteins[13,28-30] but has not been subjected to a systematic examination using a benchmark of a series of related reactions.

The present study evaluates the solute and solvent reorganization energies (λ_S and λ_s, respectively) and indicates that the λ_s obtained by the phenomenological approach is quite different than the corresponding microscopic parameter. More importantly, perhaps, we demonstrate that the λ_S and λ_s obtained from microscopic simulation and the corresponding quantum mechanical nuclear corrections can reproduce the observed LFER for a series of six reactions with a single adjustable parameter that determines the off-diagonal matrix element.

In Section 2 we describe our theoretical approach. The corresponding results are described in Section 3 and the significance of our finding is discussed in Section 4.

2. Methods

A reliable modeling of the energetics and dynamics of HT reactions in solution is far from trivial. Several hybrid quantum/classical methods can provide useful strategies,[1-12] but at present we believe that the EVB approach offers the best option in particular when one is interested in relating the simulations to observed LFER for a series of reactions and in obtaining clear physical interpretation to the effect of the solvent on such relationships. In our specific case we would like to consider HT reactions in the series of molecules listed in Figure 1. The EVB method describes such systems in terms of their most important resonance structures (RS's). For example, in the case of HT between molecule 1 and 2, we can describe the system in terms of the resonance structures of Figure 2a. These involve a relatively large number of combinations of the donor and acceptor RS's (e.g. (a + e), (a + f), (b + e), (b + f), (c + e), (c + f) for the RS's that contribute most to the reactant region of the potential surface). However, one can use a much smaller set of effective diabatic configurations by projecting all the RS's of the system on a subspace that reflects the asymptotic properties of the product

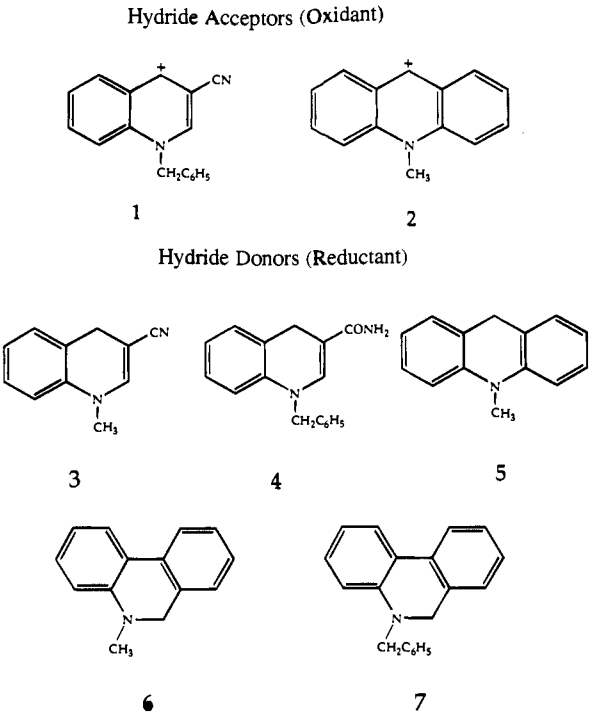

Figure 1. The molecules involved in the hydride transfer reactions.

and reactant states (see Appendix of ref 33). Thus, we can represent the main chemical aspects of our system by constructing the two configurations of Figure 2b from the RS's of Figure 2a, where the first configuration represents the lowest energy eigenvectors obtained by mixing all the RS's that represent the reactant region while the second represents the lowest energy eigenvector by mixing the RS's that describe the product state. The effective Hamiltonian of the system of Figure 2b in the gas phase is now described by

$$H_{11} = \Delta M(b_1) + {}^1/_2\sum_m K^{(1)}_{b,m}(b^{(1)}_m - b^{(1)}_{0,m})^2 + {}^1/_2\sum_m K^{(1)}_{\theta,m}(\theta^{(1)}_m - \theta^{(1)}_{0,m})^2 + K_{\chi,1}(\chi_1 - \chi_0)^2 + V^{(1)}_{QQ} + V^{(1)}_{nb} + \alpha_1 \quad (1)$$

$$H_{22} = \Delta M(b_2) + {}^1/_2\sum_m K^{(2)}_{b,m}(b^{(2)}_m - b^{(2)}_{0,m})^2 + {}^1/_2\sum_m K^{(2)}_{\theta,m}(\theta^{(2)}_m - \theta^{(2)}_{0,m})^2 + K_{\chi,2}(\chi_2 - \chi_0)^2 + V^{(2)}_{QQ} + V^{(2)}_{nb} + \alpha_2$$

$$H_{12} = A_{12}e^{-\mu r_3}$$

where $\Delta M(b_m)$ denotes a Morse potential (relative to its minimum for the bond m in the ith resonance structure). The b_m, θ_m, and χ_m terms are the bond, angle, and out-of-plane bending contributions, respectively. The bond lengths involved directly in the reaction (b_1 and b_2) are defined in Figure 2b. χ_1 and χ_2 are respectively the out-of-plane angles of the donor and acceptor carbon (the corresponding terms appear when the given carbon is in sp^2 hybridization). $V^{(1)}_{QQ}$ is the Coulombic interaction between the charges for resonance structure i, and $V^{(i)}_{nb}$ is the nonbonded interaction between the atoms of this resonance structure. The distance r_3 is also defined in Figure 2b. The parameters used for the different terms (except the α's) in H_{11} and H_{22} are the same parameters used in ref 18.

The EVB Hamiltonian for the system in solution is given by[1,5]

$$H^s_{ii} = H_{ii} + V_{Ss} + V_{ss} \quad (2)$$

$$H^s_{12} = H_{12}$$

where V_{Ss} represents the interaction potential between the solute (S)

(24) Bader, J. S.; Kuharski, R. A.; Chandler, D. *J. Chem. Phys.* **1990**, *93*, 230.
(25) Zheng, J. A.; McCammon, C.; Wolynes, P. G. *Chem. Phys.* **1991**, *158*, 261.
(26) Gillan, M. J. *J. Phys. C: State Phys.* **1987**, *20*, 3621.
(27) Voth, G. A.; Chandler, D.; Miller, W. H. *J. Chem. Phys.* **1989**, *91*, 7749.
(28) Warshel, A.; Chu, Z. T. *J. Chem. Phys.* **1990**, *93*, 4003.
(29) Hwang, J.-K.; Chu, Z. T.; Yadav, A.; Warshel, A. *J. Phys. Chem.* **1991**, *95*, 8445.
(30) Hwang, J.-K.; Warshel, A. *J. Phys. Chem.* **1993**, *97*, 10053.
(31) (a) Wonchoba, S. E.; Truhlar, D. G. *J. Chem. Phys.* **1993**, *99*, 9637. (b) Truhlar, D. G.; Liu, Y.-P.; Schenter, G. K.; Garrett, B. C. *J. Phys. Chem.* **1994**, *98*, 8396.
(32) Kreevoy, M. M.; Ostovic, D.; Lee, I.-S. H.; Binder, D. A.; King, G. W. *J. Am. Chem. Soc.* **1988**, *110*, 524.
(33) Warshel, A.; Russell, S. T. *J. Am. Chem. Soc.* **1986**, *108*, 6570.

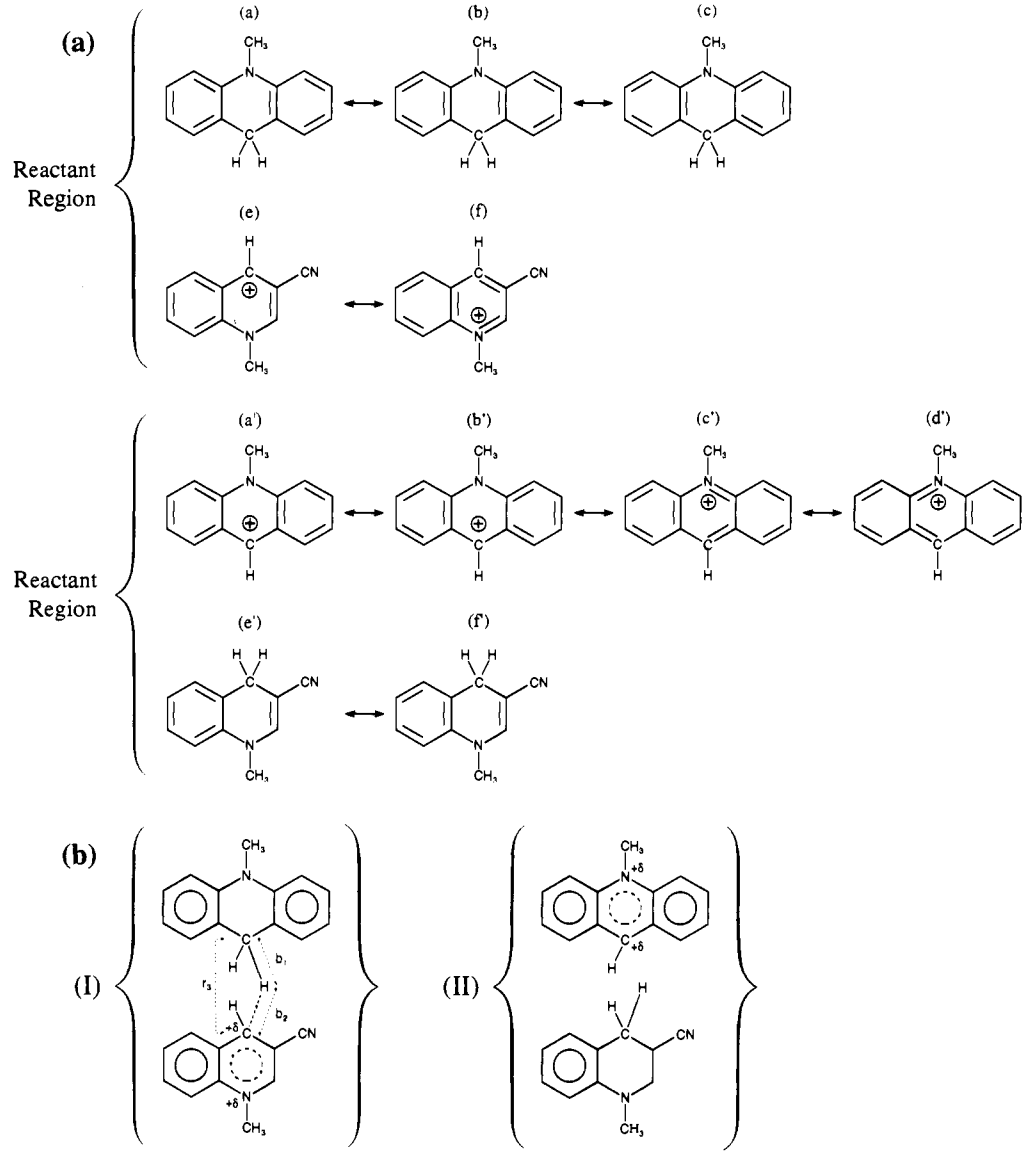

Figure 2. (a) The relevant resonance structure involved in the description of reaction 1. (b) The effective two-resonance structures that are used to describe the energetics of reaction 1. The same type of structures are used in all other reactions.

and the solvent (s) while V_{ss} represents the interaction between the solvent molecules (see ref 5 for details). The potential functions and parameters used for the solute–solvent and solvent–solvent interaction terms are the standard parameters of the ENZYMIX program.[34]

In principle, one can obtain the gas-phase matrix elements by VB *ab initio* treatments (e.g., ref 35). Another approach is to perform MO based *ab initio* calculations for several points along the reaction coordinate in the gas phase and then to adjust H_{ij} and H_{ii} so that the calculated ground state obtained from diagonalizing the EVB gas-phase Hamiltonian reproduces the *ab initio* energy surface (see refs 5 and 36 for examples). However, here and in many other cases, we prefer to accomplish this task by using information about the reaction in solution. In particular it is very useful to obtain the gas-phase-shift parameters (the α_i) by using the observed $\Delta G°$ for the solution reaction together with the calculated solvation free energies of the reacting fragments at infinite separation (see refs 1 and 5). This is done in our specific case by adjusting $(\alpha_2 - \alpha_1)$ until the calculated and observed values of $\Delta G°$ coincide (see Results section). The determination of the α_i from the experimental information about the isolated fragments in solution is in fact equivalent to recalibration or examination of the asymptotic energies, which is an essential step of any other sensible quantum mechanical approach, except that the EVB provides a natural way for this calibration. Once the calibrated α's are obtained we are left with the need to evaluate H_{12}. As pointed out above, this can be done by gas-phase *ab initio* calculations but in the present work we will consider H_{12} as the only truly adjustable parameter in our treatment (using, however, a single functional form for the H_{12} of all reactions considered). It is hoped that combining this approach with the corresponding quantum mechanical corrections to the rate constants will allow us to account for the observed LFER. This should amount to a reproduction of the observed experimental results using λ_s and λ_s that are determined by a first principle microscopic approach rather than deducing these parameters in a phenomenological way.

The evaluation of the free energy functions and the corresponding reorganization energies is accomplished in a straightforward way by the EVB formulation. This is done by the previously developed FEP/umbrella-sampling method.[5] This model uses a mapping potential of the form[1c]

$$V_m = H_{11}(1 - \theta_m) + H_{22}\theta_m \tag{3}$$

where the change of θ_m from zero to one drives the system from the reactant to the product state. The classical free energy function is given by[1,5]

(34) Lee, F. S.; Chu, Z. T.; Warshel, A. *J. Comput. Chem.* **1993**, *14*, 161.

(35) Bernardi, F.; Olivucci, M.; Robb, M. A. *J. Am. Chem. Soc.* **1992**, *114*, 1606.

(36) Chang, Y. T.; Miller, W. H. *J. Phys. Chem.* **1990**, *94*, 5884.

$$\exp\{-g(X)\beta\} = \exp\{-\Delta G(\theta_m)\beta\} \times \langle\delta(X - X')\exp\{-(V_g - V_m)\beta\}\rangle_{V_m} \quad (4)$$

here $\beta = (k_B T)^{-1}$ (k_B is the Boltzmann constant), and $\Delta G(\theta_m)$ is the free energy associated with changing θ from zero to θ_m evaluated by a standard FEP approach.[1,5] θ_m is the θ that forces the system to spend most time near the given X'. V_g is the adiabatic ground state obtained by solving the secular equation $\mathbf{HC} = V_g\mathbf{C}$, and X is the hypersurface of constant energy gap between the diabatic surface, i.e., $X' = H_{22} - H_{11}$ = constant. $\langle\ \rangle_{V_m}$ designates an average over trajectories with the mapping potential V_m.

In addition to evaluating $\Delta g(X)$ one can obtain the probability of being at the given X on H_{11} or H_{22}. The corresponding free energy functions are given by[1,5]

$$\exp\{-g_i(X)\beta\} = \exp\{-\Delta G(\theta_m)\beta\} \times \langle\delta(X - X')\exp\{-(H_{ii} - V_m)\beta\}\rangle_{V_m} \quad (5)$$

With the calculated g, g_1, and g_2, we can describe each reaction using diagrams of the type depicted in Figure 3. This type of diagram can be used to obtain the reorganization energy (λ), which is given by the energy released upon placing the system on the potential surface of state 2, with the equilibrium coordinates of state 1, and then letting it relax to the equilibrium coordinates of state 2. This reorganization energy is depicted schematically in Figure 3. This figure also describes the diabatic activation energy, $\Delta g^{\ddagger}$, obtained by $g_1(X^{\ddagger}) - g_1(X_1^0)$ and the adiabatic activation free energy obtained from the difference between the maximum of the g curve and its minimum at the reactant region. Using the calculated $\Delta g^{\ddagger}$ we can calculate the classical rate constant, using[5]

$$k_{cl} = F(k_B T/h)\exp\{-\Delta g^{\ddagger}\beta\} \quad (6)$$

where F is the transmission factor obtained by running downhill trajectories from the transition state (see ref 5). Here, however, we assume that F is close to 1, which is a reasonable approximation in cases of large $\Delta g^{\ddagger}$.[1a]

In order to evaluate the quantum mechanical rate constant we use the approximation (see refs 26 and 27)

$$k_{qu} = k_{cl}\exp\{-\Delta\Delta g^{\ddagger}_{cl\to qu}\beta\} \quad (7)$$

where $\Delta\Delta g^{\ddagger}_{cl\to qu}$ is the difference between the quantum and classical activation free energy. Our approach for evaluation of $\Delta\Delta g^{\ddagger}$ is based on the recently developed quantized classical path (QCP) approach. This approach evaluates the quantum mechanical activation energy by propagating trajectories of the classical particles and using these trajectories to generate the centroid positions for the quantum mechanical partition function. This treatment is based on the finding[30] that the quantum mechanical partition function can be expressed as

$$Z_{qu} = Z_{cl}\left\langle\left\langle\exp\left\{\frac{-\beta}{p}\sum_k (V(x_k) - V(\bar{x}))\right\}\right\rangle_{fp}\right\rangle_V \quad (8)$$

where V is the given potential surface and each classical particle is represented by p quasiparticles with coordinates (x_1, x_2, ... x_p) and $\bar{x}$ is the center of gravity (centroid) of these particles. $\langle\ \rangle_{fp}$ designates an average over the free particle distribution constrained at $\bar{x}$ while $\langle\ \rangle_V$ designates an average over classical trajectories on the potential V. Using eq 8, one can express the quantum mechanical free energy surface[29,30] by

$$\exp\{-\Delta g(X)_{qu}\beta\} = \exp\{-\Delta G(\theta_m)_{cl}\beta\} \times \left\langle\delta(X - \bar{X})\left\langle\exp\left\{-\left(\frac{\beta}{p}\right)\sum_k (V_g(x_k) - V_m(\bar{x}))\right\}\right\rangle_{fp}\right\rangle_{V_m} \quad (9)$$

where $\bar{X}$ designates the hypersurface of constant energy gap between the diabatic surfaces, i.e., $\bar{X} = H_{22}(\bar{x}) - H_{11}(\bar{x})$ = constant. V_m is the mapping potential of eq 3 and V_g is the adiabatic ground state potential.

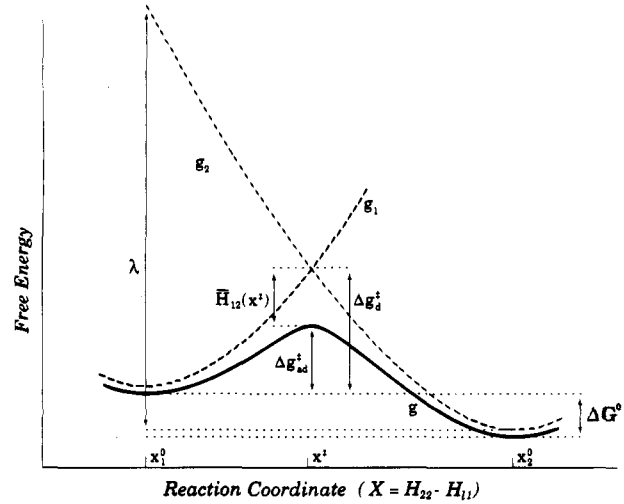

Figure 3. Schematic description of the relationship between the diabatic and adiabatic free energy functions and the corresponding activation energies and reorganization energies.

Table 1. Reactions Studied in the Present Work

reaction no.	donor	acceptor
1	**3**	**2**
2	**5**	**1**
3	**4**	**2**
4	**7**	**2**
5	**6**	**2**
6	**6**	**1**

The activation energy $\Delta g^{\ddagger}_{qu}$ is obtained from the difference between the maximum and minimum of the $\Delta g(X)_{qu}$ curve. Our treatment is related to the centroid formulation of Gillan[26] and Voth et al.[27] but it uses classical trajectories as an effective and convenient way for evaluation of the quantized $\Delta g(X)$. More specifically, centroid simulations evaluate trajectories of the $n \times p$ quasiparticles (where n is the number of classical coordinates) and collect the contribution to the quantum activation energy wherever the $\bar{X}(\bar{x})$ coincide with the specific value of the reaction coordinate X. On the other hand, the QCP method evaluates the trajectories of the classical particles under the potential V_m and then obtains the quantum average of eq 9 by integrating the motion of the quasiparticles, considering only the effect of the free particle potential. This treatment does not require evaluation of forces $\delta V_m/\delta x_k$ during the quantum calculations. Furthermore, the *fp* average can be performed in larger time intervals than that needed by the classical trajectories. The QCP approach has been used before in studies of model systems[30] and in actual simulation of proton transfer and hydrid transfer reactions in solutions and proteins.[13,29,30]

3. Results

Using the methods described above, we perform simulation studies of the hydride transfer reactions listed in Table 1. The simulations were done using the program ENZYMIX[34] with the surface constrained all atom solvent (SCAAS) spherical boundary conditions. This involved a construction of a water sphere of 10 Å radius (with about 120 water molecules around the reacting molecules and special radial and polarization boundary conditions.[34] The hydride-acceptor atom was constrained to the center of the solvent sphere and the distance between the hydride-donor and hydride-acceptor atoms was constrained to 3.0 Å with a weak quadratic function ($V' = 10(r_3 - r_3^0)^2$ kcal mol^{-1} Å^{-2}). The calculations were done without any interaction cutoff between the molecules within the simulation sphere. The FEP/umbrella-sampling simulations were done with 11 simulation steps, changing θ_m of eq 3 from 0 to 1 in equal increments of 0.1. Each step involved a 4 ps molecular dynamic simulation with time steps of 1 fs at a temperature of 300 K. The

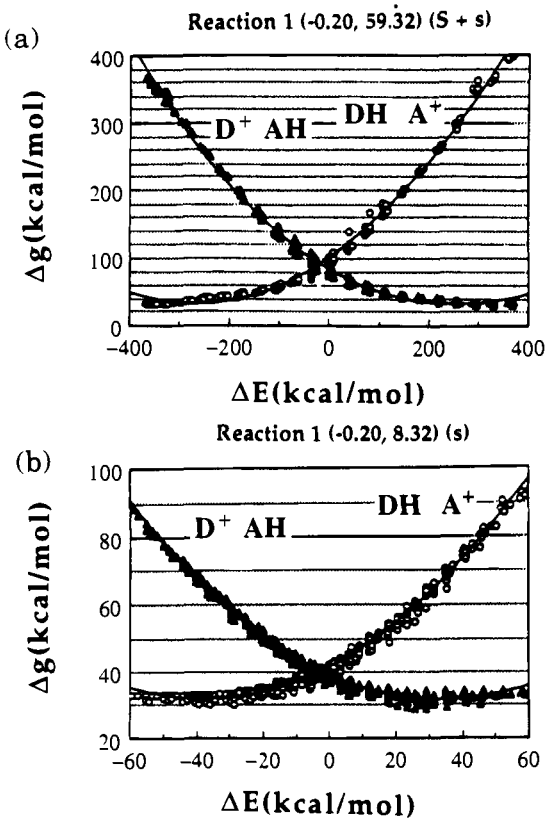

Figure 4. (a) The total (solute + solvent) free energy functions for reaction 1. The minima of the functions are set so that they reproduce the observed $\Delta G°$ and this is equivalent to finding the correct value of $\alpha_2 - \alpha_1$. The numbers in parentheses designate respectively the $\Delta G°$ and $\Delta g^{\ddagger}$ obtained from the given free energy functions. (b) The solvent contributions for the free energy functions of reaction 1. The minima of the functions are set in a way that reproduces the observed $\Delta G°$.

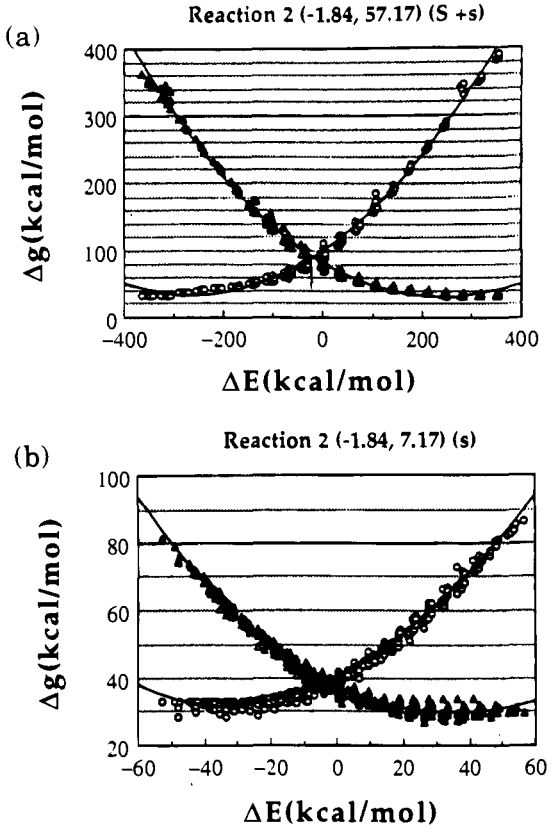

Figure 5. (a) The total (solute + solvent) free energy functions for reaction 2. Notation and procedure as in Figure 4. (b) The solvent contributions for the free energy functions of reaction 2.

simulations were repeated at five independent sets of initial conditions and the corresponding results were averaged over these runs. This averaging procedure has been found to be much more effective than running a single long trajectory (see ref 37). The parameters used for the simulation are considered in the Methods section except that the values of $\alpha_2 - \alpha_1$ and H_{12} will be considered below.

Using the above simulation procedure we evaluated the classical free energy functions for our series of six hydride transfer reactions. The evaluation of those functions involved the collection of the data points for the $g_i(X)$ of eq 5 and the fitting of a polynomial to these points (e.g., see Figure 4) to obtain the analytical description of the given function (see ref 14 for a related procedure). The different free energy functions were evaluated with and without the solute contribution (Figures 4–9). The corresponding reorganization energies for both the solute + solvent (λ_{S+s}) and solvent (λ_s) were determined in each case from the difference between the value of the free energy function of the product state at the minimum of the free energy function of the reactant state and the value of the product free energy function at its own minimum (see Figure 3 and the discussion in the Methods section). The values of the calculated reorganization energies for the six reactions are summarized in Table 2. It might be useful to point out that the calculations appear to provide quite reliable estimates of the solvent reorganization energies (we estimate the convergence error to be around ±2 kcal/mol). This is of significant importance since one cannot expect to have the same reorganization energies for all the reactions studied[32] and it is hard to evaluate the relevant parameters in a unique way using experimental information. Thus the present study as well as earlier studies[14-16] demonstrate the great value of computer simulation approaches in the determination of reorganization energies.

After evaluating the shapes of the free energy functions for each reaction, we determined their relative heights by selecting the value of $\alpha_2 - \alpha_1$ that forces the difference between the minima of the product and reactant free energy functions to reproduce the observed $\Delta G°$ (see Figure 3). This procedure provides a unique calibration of $\alpha_2 - \alpha_1$ that allows one to determine the diabatic activation free energy, $\Delta g_d^{\ddagger}$, from the intersection of the reactant and product free energy functions (see Figure 3), although a somewhat improved estimate can be obtained when the value of $\alpha_2 - \alpha_1$ is adjusted so that the calculated adiabatic $\Delta G°$ reproduces the corresponding observed value, but in the present case the two procedures give similar results. The calculated values of the diabatic free energies are summarized in Table 3. These values allow us to examine whether the calculated free energy curves can be approximated by quadratic functions. This is done here by comparing the values of the diabatic free energies, $\Delta g_d^{\ddagger}$, to the corresponding approximated values obtained by the Marcus formula

$$\Delta g_{d,M}^{\ddagger} = \frac{(\Delta G° + \lambda)^2}{4\lambda} \tag{10}$$

where d and M designate diabatic and Marcus, respectively. The analysis presented in Table 3 and Figure 10 indicates that $\Delta g_{d,M}^{\ddagger}$ provides an excellent approximation for $\Delta g_d^{\ddagger}$. Since eq 10 is simply the result obtained from the intersection of two harmonic functions with equal curvature, we conclude that the calculated free energy functions can be approximated by

(37) Lee, F. S.; Warshel, A. *J. Chem. Phys.* **1992**, *97*, 3100.

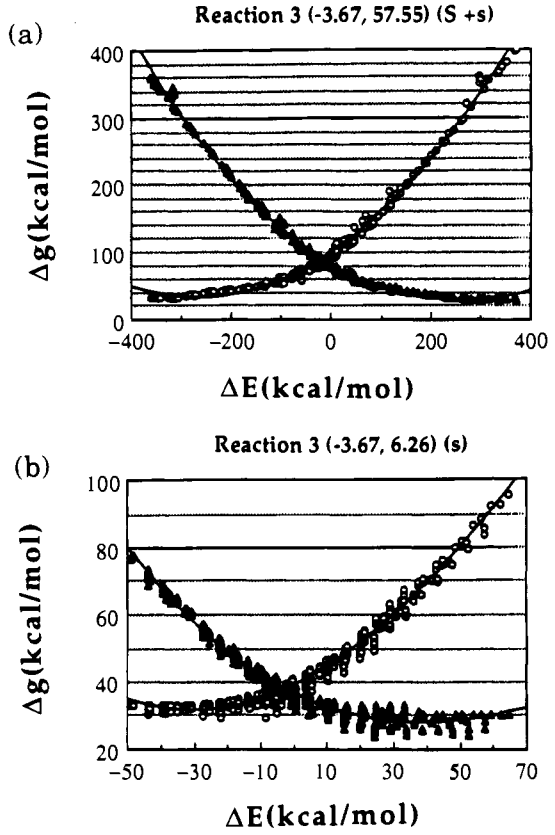

Figure 6. (a) The total (solute + solvent) free energy functions for reaction 3. Notation and procedure as in Figure 4. (b) The solvent contributions for the free energy functions for reaction 3.

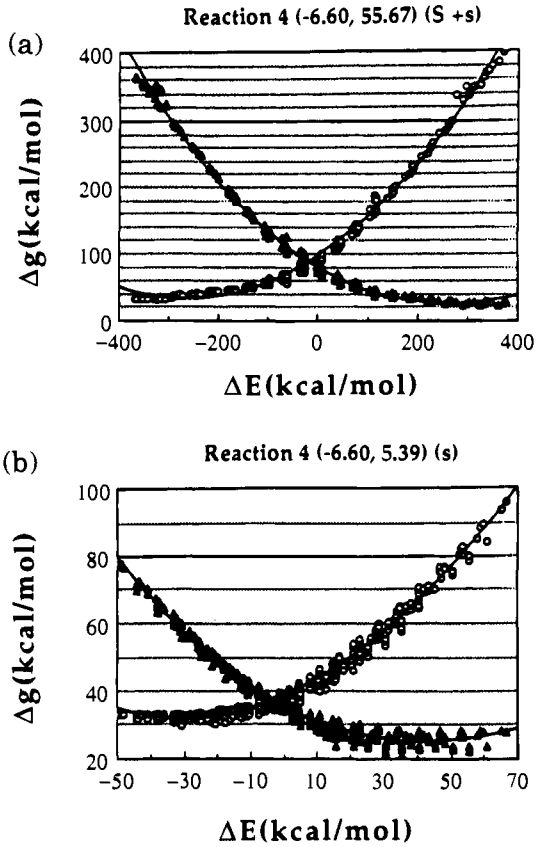

Figure 7. (a) The total (solute + solvent) free energy functions for reaction 4. Notation and procedure as in Figure 4. (b) The solvent contributions for the free energy functions for reaction 4.

harmonic functions (this is also evident from the polynomial fitting procedure) and that our system follows the linear response approximation for both the solvent and the combined solute + solvent contributions.

After analyzing the diabatic free energy functions we examined the adiabatic free energy functions and the corresponding activation free energies. This step of our analysis involves the evaluation of the classical and quantum mechanical adiabatic free energies for different assumed values of the parameters A and μ in the H_{12} of eq 1. The classical adiabatic free energy functions were evaluated in the same simulations used for the determination of the g_i using, however, eq 4 instead of eq 5. The quantum mechanical free energy functions were determined using the quantized classical path (QCP) approach. The simulations involved mapping steps of 10 ps each. The classical trajectory was propagated with 1 fs time steps and the quantum average over the free particle potential was done once in every 10 fs. The quantum calculation used 40 quasiparticles ($p = 40$ in eq 8) for each of the EVB quantum atoms. The propagation of the quasiparticle was done as in ref 30 using Langevin dynamics. Typical results of these simulations is presented in Figure 11.

The process of optimizing H_{12} was guided by using a modified Marcus relationship[1,5] (see also Figure 3)

$$\Delta g^{\ddagger}_{qu} = \Delta g^{\ddagger}_{cl} - \Delta\Delta g^{\ddagger}_{cl\rightarrow qu} \cong (\lambda + \Delta G^{\circ})^2/4\lambda - \{H_{12}(X^{\ddagger}) - H^2_{12}(X_0)/(\lambda + \Delta G^{\circ})\} - \Delta\Delta g^{\ddagger}_{cl\rightarrow qu} \quad (11)$$

where $X^{\ddagger}$ and X_0 are respectively the maximum and minimum of the free energy function of the reactant state. Using the average value of the calculated λ and the observed $\Delta g^{\ddagger}$ and ΔG° we obtain

$$H_{12}(X^{\ddagger}) - H^2_{12}(X_0)/(\lambda + \Delta G^{\circ}) - \Delta\Delta g^{\ddagger}_{cl\rightarrow qu} = 29 \text{ kcal/mol} \quad (12)$$

The parameters A and μ in H_{12} were optimized by trying to satisfy eq 12. The optimal H_{12} was found to be

$$H_{12}(r_3) = 150 \exp\{-0.5 r_3\} \text{ kcal/mol} \quad (13)$$

With this H_{12} we obtained $\Delta\Delta g^{\ddagger}_{cl\rightarrow qu} = -5.9$ kcal/mol for reaction 1 (see Figure 11) and a similar value for reaction 2. This and the average value of λ_{S+s} (i.e. $\lambda_{S+s} \simeq 236$ kcal/mol), as well as $H_{12}(X^0) = H_{12}(r_3^0 = 3.0) = 33.5$ kcal/mol and $H_{12}(X^{\ddagger}) = H_{12}(r_3{=}2.75) = 37.9$ (where r_3^0 and $r_3^{\ddagger}$ are the average values of r_3 at X^0 and $X^{\ddagger}$, respectively), satisfy eq 12. As is seen from Figure 10 we obtained a good agreement between the calculated and observed $\Delta g^{\ddagger}$ using the single H_{12} of eq 12.

4. Concluding Remarks

This work has examined the molecular basis for the observed LFER for HT reactions in solutions, using microscopic simulation methods. It was demonstrated that the free energy functions can be approximated by harmonic functions and that this linear response approximation is valid not only for the solvent contribution but also for the solute contribution.

The fact that the free energy functions are harmonic indicates that the LFER of the given class of reactions can be described by the modified Marcus relationship of eq 11. Yet, in contrast to the case of electron transfer and other diabatic reactions, it is hard to deduce the relevant reorganization energies by

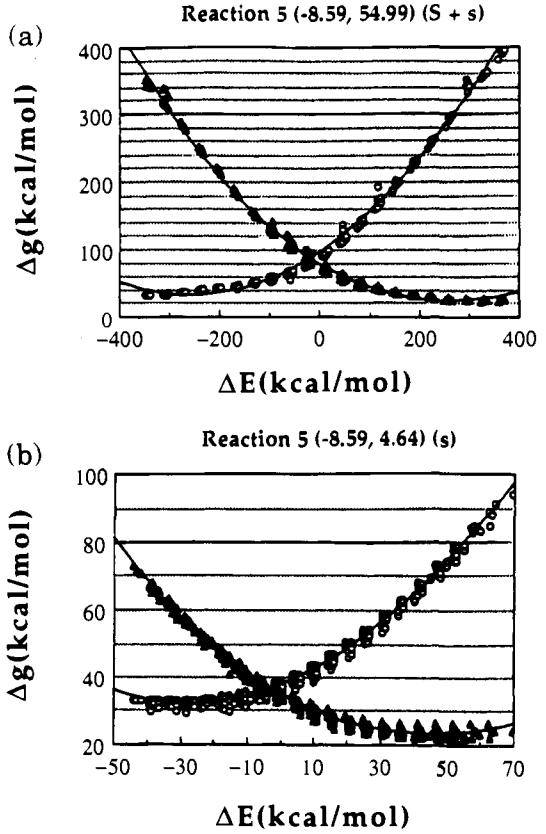

Figure 8. (a) The total (solute + solvent) free energy functions for reaction 5. Notation and procedure as in Figure 4. (b) The solvent contributions for the free energy functions for reaction 5.

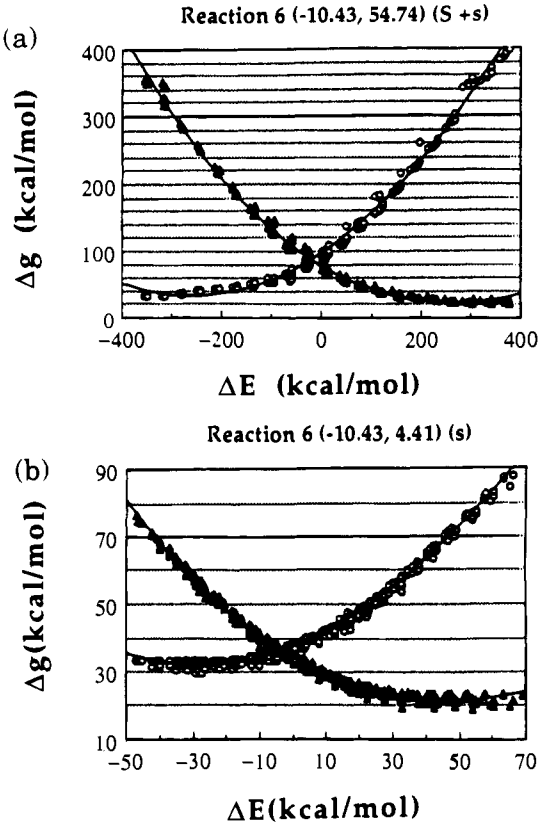

Figure 9. (a) The total (solute + solvent) free energy functions for reaction 6. Notation and procedure as in Figure 4. (b) The solvent contributions for the free energy functions for reaction 6.

Table 2. Calculated λ's and the Corresponding Observed $\Delta G°$'s

reaction no.	λ_{s+s}	λ_s	$\Delta G°$
1	237.6	33.7	−0.2
2	232.4	32.9	−1.8
3	237.6	32.3	−3.7
4	235.8	33.9	−6.6
5	237.1	34.3	−8.0
6	239.0	35.9	−10.4

phenomenological procedures. In fact, the λ_s obtained by the simulations ($\lambda_s \simeq 33$ kcal/mol) is much smaller than the empirical value obtained by fitting the diabatic Marcus relationship to the observed LFER ($\lambda_{fit} \simeq 80$). This reflects the important contribution of the solute reorganization energy. It is also important to note that the total reorganization energy obtained by the present treatment ($\bar{\lambda} \simeq 236$ kcal/mol) is much larger than the phenomenological λ. This discrepancy is due to the effect of H_{12} and the quantum mechanical correction. That is, the contributions of H_{12} and $\Delta g_{cl\to qu}$ reduce $\Delta g^{\ddagger}$ by about 40 kcal/mol, thus decreasing the apparent λ by $4 \times 40 =$ 160 kcal/mol, and bringing it to 76 kcal/mol, in good agreement with the phenomenologically deduced λ.

The present study evaluated the quantum mechanical correction to the rate constant of a hydride transfer reaction in solution using realistic potential surfaces and the QCP approach. Another variant of this approach has been used in preliminary studies of isotope effects of hydride transfer reaction in the enzyme LDH.[29] These studies have demonstrated the effectiveness of the QCP method in simulations of hydride transfer reactions in condensed phases but have not established the reliability of this method. More systematic studies (which are left to subsequent works) will require evaluations of isotope effects in hydride transfer between NAD^+ analogues and comparison to the corresponding calculated and observed results. In particular, it would be interesting to analyze the observed solvent effect on this class of reactions.[38] It would also be interesting to refine H_{12} using gas phase *ab initio* calculations and to reexamine the absolute value of $\Delta g^{\ddagger}_{cl\to qu}$, as well as the relationship between the EVB results obtained with realistic surfaces and those obtained with more phenomenologically deduced potential surfaces.[39]

Perhaps the most significant finding of the present work is the fact that a single adjustable H_{12} can reproduce the observed LFER in a series of six hydride transfer reactions and that this was done with a fully microscopic simulation approach without assuming *a priori* any Marcus-like relationship. This provides further evidence for the effectiveness of the EVB method in describing and analyzing chemical processes. In fact, as was pointed out repeatedly by us,[1] the EVB does not assume any LFER or parabolic free energy function, but reproduces such behavior as a consequence of the tendency of multidimensional systems to satisfy the linear response approximation.[14] The extremely useful picture provided by applying the VB representation to chemical processes of polyatomic molecules (e.g. refs 1 and 40) has also been emphasized by Shaik and co-workers (e.g. ref 41), who used an approach which is conceptually similar to the EVB model but much less quantitative and thus is not amenable to verification by microscopic simulations.

(38) Kreevoy, M. M.; Kotchevar, A. T. *J. Am. Chem. Soc.* **1990**, *112*, 3579.

(39) (a) Kreevoy, M. M.; Ostovic, D.; Truhlar, D. G.; Garrett, B. C. *J. Phys. Chem.* **1986**, *90*, 3766. (b) Kim, Y.; Truhlar, D. G.; Kreevoy, M. M. *J. Am. Chem. Soc.* **1991**, *113*, 7837.

(40) Warshel, A.; Weiss, R. M. *J. Am. Chem. Soc.* **1980**, *102*, 6218.

(41) Pross, A.; Shaik, S. S. *Acc. Chem. Res.* **1983**, *16*, 363.

Table 3. Activation Free Eneriges Obtained by Different Approaches[a]

reaction no.	*A*	*B*	*C*	*D*	*E*	*F*	*G*	*H*	*I*
1	59.31	8.32	59.32	8.32	59.08	8.33	20.32	20.07	19.73
2	57.18	7.20	57.17	7.17	58.26	7.54	18.18	19.26	19.27
3	57.57	6.34	57.55	6.26	57.36	6.70	18.55	18.35	17.52
4	55.72	5.49	55.67	5.39	55.92	5.46	16.67	16.92	16.54
5	55.05	4.81	54.99	4.64	54.96	4.69	15.99	15.96	16.01
6	54.82	4.52	54.74	4.41	54.08	4.02	15.74	15.08	16.26

[a] *A*, diabatic activation free energies ($\Delta g_{d,M}^{\ddagger}$) determined by using the Marcus relationship with λ_{S+s}. *B*, diabatic activation free energies determined by using the Marcus relationship with λ_s. *C*, diabatic activation free energies ($\Delta g_d^{\ddagger}$) determined from the intersection of the free energy functions. *D*, diabatic activation free energies determined from the intersection of the solvent free energy functions. *E*, diabatic activation free energies ($\Delta g^{\ddagger}$) determined by using the Marcus relationship with the average values of $\lambda_{S+s}/4$. *F*, diabatic activation free energies determined by using the Marcus relationship with the average values of $\lambda_s/4$. *G*, adiabatic activation free energies obtained by subtracting 39 kcal/mol from the corresponding $\Delta g_d^{\ddagger}$ of column *C*. *H*, adiabatic activation free energies obtained by subtracting 39 kcal/mol from the $\Delta g_M^{\ddagger}$ of column *E*. *I*, observed activation free energies.

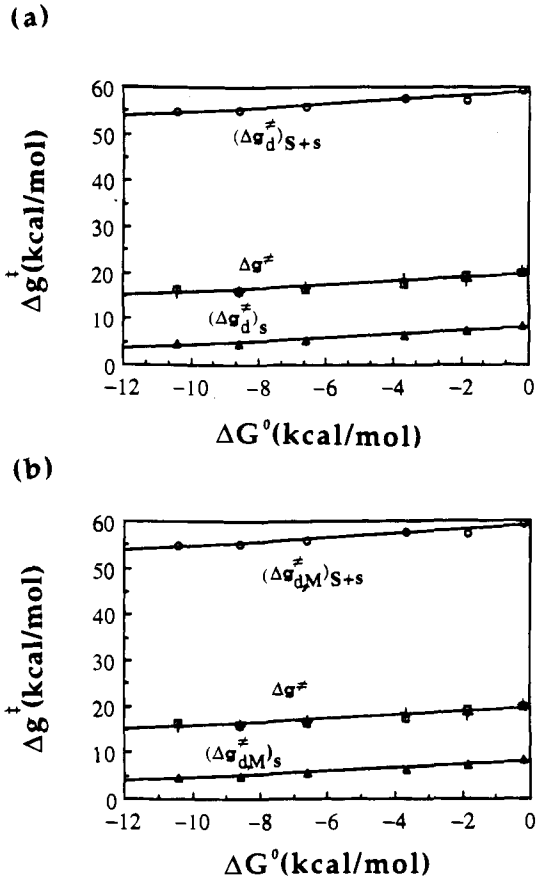

Figure 10. Calculated and observed LFER for the six hydride transfer reactions studied in this work. (a) The LFER evaluated using the calculated free energy functions. The diabatic activation free energies, $\Delta g_d^{\ddagger}$, obtained using the solute + solvent and the solvent contributions are designated by ○ and △, respectively. The adiabatic activation free energies, $\Delta g^{\ddagger}$, obtained by subtracting 39 kcal/mol from the $\Delta g_d^{\ddagger}$ are designated with a + sign and compared to the corresponding observed values (designated by □). (b) The LFER evaluated using the Marcus relationship and the microscopically derived reorganization energies. The diabatic activation free energies, $\Delta g_d^{\ddagger}$, obtained from the Marcus relationship are designated by ○ and △, respectively. The adiabatic activation free energies, $\Delta g^{\ddagger}$, obtained by subtracting 39 kcal/mol from the $\Delta g_d^{\ddagger}$ are designated with a + sign and compared to the corresponding observed values (designated by □).

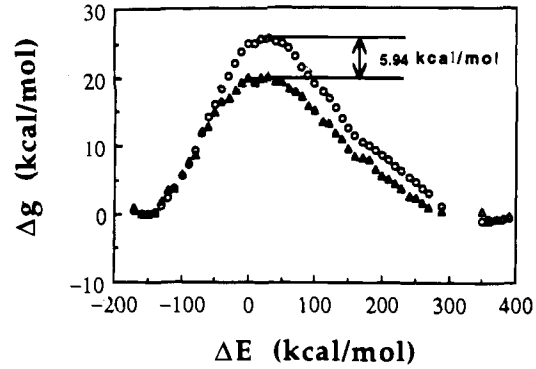

Figure 11. The classical (○) and quantum mechanical (△) adiabatic free energy curves for reaction 1. The quantum mechanical free energy curve was obtained by the QCP approach.

Quantitative studies of medium sized molecules in solutions present a major challenge. Significant progress has been made by phenomenological approaches but probably the only way to progress toward quantitative understanding is to simulate the detailed molecular event during the given reaction using realistic molecular models. *Ab initio* approaches can help in this respect by providing information about the relevant gas phase process, and in fact, such approaches have been used successfully in studies of hydride reactions (e.g. refs 42–44). The problem is, however, that we are interested in reactions in solutions and proteins where environmental effects must be incorporated into the given model. The simplest (zero-order) option would be to evaluate the *ab initio* charges at different points along the gas phase reaction path and to add the corresponding solvation energies to the gas phase energies (see for example ref 4). This approach does not reflect, however, the polarization of the solute by the solvent and can lead to quite incorrect results in studies of charge separation processes (see discussion in ref 5). A very effective option of capturing the physics of the solute polarization is provided by the EVB method. One can easily obtain an EVB Hamiltonian that is calibrated to reproduce the gas phase energy surface and charge distribution. Solvating the gas state EVB charges will obviously reproduce the above zero-order results. On the other hand, solvating the diabatic states by using eq 2 and then mixing them (as done in the standard EVB procedure) will provide a model that clearly accounts for the main features of solvent-induced solute polarization, where stabilization of ionic states increase their contribution to the ground state charge distribution. Such a model would reproduce the exact results at the asymptotic regions (which is not necessarily the case for the zero-order model and for MO models without a configuration interaction treatment). In the non-asymptotic region the model can be further refined by calibrating it to reproduce the response of the gas phase charges to external fields. Thus the EVB method provides what is perhaps the most

(42) Wu, Y.; Houk, K. N. *J. Am. Chem. Soc.* **1987**, *109*, 906.
(43) Wu, Y.; Houk, K. N. *J. Am. Chem. Soc.* **1987**, *109*, 2226.
(44) Tapia, O.; Andres, J.; Aullo, J. M.; Branden, C. I. *J. Chem. Phys.* **1985**, 83.

effective way of interpolating gas phase *ab initio* results in physically meaningful calculations of solution reactions. In cases where the *ab initio* results are not reliable enough one may use results from solution experiments and calculated solvation energies to calibrate the gas phase Hamiltonian. Of course, eventually one will be able to obtain reliable results for solution reactions using well-calibrated hybrid *ab initio*/classical methods, but the simple physical picture of the EVB would still be very useful in analyzing the trend in activation energies and their quantum mechanical corrections as well as in understanding the effect of the solvent on these properties. For example, one can use the EVB and QCP approaches in analyzing the observed effect of solvents with different dielectric relaxation time on the isotope effect of hydride transfer reactions.[38]

Finally, considering the fact that the present study has demonstrated the ability of the EVB method to reproduce quantitatively the observed trend in hydride transfer reactions in solution, it seems reasonable to assume that this method should give reliable results in studies of hydride transfer reactions in enzymes.

Acknowledgment. This work was supported by Grant No. GM 24492 from the National Institutes of Health.

JA9500769